Available online at www.sciencedirect.com

ScienceDirect

Current Opinion in
Colloid & Interface Science

Cyclization reactions in confined space

Emanuele Spatola, Federico Frateloreto, Daniele Del Giudice, Giorgio Olivo and Stefano Di Stefano

Abstract

Cyclization of chain substrates into ring products is an important reaction in organic synthesis. The ease of this process is measured by the Effective Molarity, which indicates that some rings (5, 6 and 7-membered ones) are especially facile to close, while others (>8 membered) are far more challenging. Confinement of the cyclization inside the nanometric cavity of capsules, coordination cages or porous materials can greatly facilitate the reaction via preorganization of the reagents and stabilization of the transition states, also offering the chance to alter the innate selectivity of the reaction. Moreover, the use of chiral cavities enables control over cyclization stereoselectivity. Eventually, pre-organization of the substrate chain inside the cavity can facilitate the closure of medium and large rings, a longstanding goal in organic synthesis. This review analyzes examples of the use of nanoconfinement to improve cyclization reactions, control their selectivity and close challenging rings.

Addresses

Dipartimento di Chimica, Università di Roma La Sapienza and ISB-CNR Sede Secondaria di Roma - Meccanismi di Reazione, Piazzale Aldo Moro 5, 00185 Rome, Italy

Corresponding authors: Di Stefano, Stefano (stefano.distefano@uniroma.it); Olivo, Giorgio (giorgio.olivo@uniroma.it)

Current Opinion in Colloid & Interface Science 2023, **64**:101680

This review comes from a themed issue on Reactivity in Confined Media

Edited by **Alessandro Scarso** and **Luca Beverina**

For a complete overview see the Issue and the Editorial

https://doi.org/10.1016/j.cocis.2023.101680

1359-0294/© 2023 Elsevier Ltd. All rights reserved.

Keywords

Cyclization, Confined space, Supramolecular catalysis, Cage, Macrocyclization.

Introduction

A cyclization reaction is defined as "the formation of a ring compound from a chain by the formation of a [single] new bond" [1]. Cyclizations have to be distinguished from "cycloaddition reactions" in which cyclic compounds are instead obtained through the contextual formation of two covalent bonds between two linear precursors [2]. In this review, we will specifically focus on cyclization reactions and on the advantages offered by their confinement in the restricted space of molecule-sized reactors such as coordination cages, capsules, cavitands or porous materials. These concave structures form cavities of nanometric size that can host and bind smaller molecules, such as linear precursors for cyclization, via supramolecular interactions. Substrate inclusion offers opportunities to facilitate a specific reaction pathway via stabilization of high-energy intermediates (and hence transition states) and/or pre-organization of the reactant(s).

Given the ubiquity of rings in organic and biological molecules, the design of effective cyclization reactions has always been a key goal in organic synthesis, and several methodologies have been developed over the years. Notwithstanding, some cyclization processes remain challenging, furnishing only low yields of the desired compound, often accompanied by substantial amounts of byproducts. Hence, new methods to facilitate challenging cyclization reactions are needed.

As recently remarked [3], a meaningful discussion concerning rates and equilibria of cyclization reactions requires a direct comparison with the related bimolecular model reactions (non-cyclization reaction operating with the same mechanism). In bulk solution, the tendency for cyclization of a bifunctional linear precursor is measured by Effective Molarity (EM), which formally is the (sometimes hypothetical) concentration of the precursor at which the cyclization rate equals the intermolecular dimerization rate [4,5]. For irreversible reactions, EM is defined by Eq (1) as the ratio between k_{intra} (the first-order kinetic constant for the cyclization of a bifunctional precursor A—B, measured in s^{-1}) and k_{inter} (the second-order kinetic constant for the corresponding bimolecular model reaction between monofunctional reactants —A and B—, measured in $M^{-1}s^{-1}$). For reversible reactions, an analogous EM is also defined, which describes the tendency of a linear precursor for cyclization under equilibrium conditions [6–8].

$$EM = k_{intra}/k_{inter} \quad (1)$$

Dedicated to Prof. Luigi Mandolini on the occasion of his 80th birthday.

The higher the EM, the greater the propensity of the linear precursor for cyclization. Operatively, if the concentration of the linear precursor A—B in bulk solution is lower than 0.1 × EM, cyclization prevails over dimerization. The magnitude of EM depends on i) the strain energy developed at the level of the cyclic transition state and ii) the number of rotors that have to be frozen or partially frozen when the linear precursor assumes the conformation of the cyclic transition state [4,5,7,8].

From a thermodynamic standpoint the EM can be considered as the product of two contributions, one enthalpic EM_H, and one entropic EM_S so that $EM = EM_H \times EM_S$ [4,5,7,8]. In the ideal case in which no strain energy is developed going from the linear precursor to the cyclic transition state ($EM_H = 1$), $EM = EM_S$ and its value can be predicted taking into account the number of rotatable bonds (r) in the linear precursor, which follows the trend depicted in Figure 1 [4,5,7–10]. If strain is developed at the transition state level, $EM_H < 1$ and enthalpic factors reduce cyclization rate and hence selectivity.

With these considerations in mind, it is possible to rationalize the ease of cyclization along a series of linear precursors composed of sp^3 carbon atoms of different chain lengths. Closing a small ring (3- and 4-membered ones) is generally feasible since the very high value of EM_S ($>10^4$ M, $r = 2$ and 3, respectively) usually overcomes the strain energy ($EM_H << 1$) developed at the cyclic transition state level. Closing common rings (5-, 6- and 7- membered ones) is facile due to a still high value of EM_S (10^1–10^3M, $r = 4$, 5 and 6, respectively) coupled to low strain ($EM_H \leq 1$). In contrast, cyclization of medium rings (8- to 11- membered rings) is challenging because the low values of EM_S ($\leq$1 M, r = from 7 to 10, respectively) do not compensate the high strain developed ($EM_H << 1$), which is largely due to transannular Prelog interactions [11]. Insertion of sp^2 carbon atoms or heteroatoms in the skeleton of the linear precursor may relieve such strain [4,5,7], but the closure reaction can be still very hard to achieve. Eventually, cyclization of large rings (12-membered and larger) is a challenging process that always requires high dilutions mainly for the low EM_S values ($\leq$0.1 M, r = 11 and higher) [4,5].

Figure 1

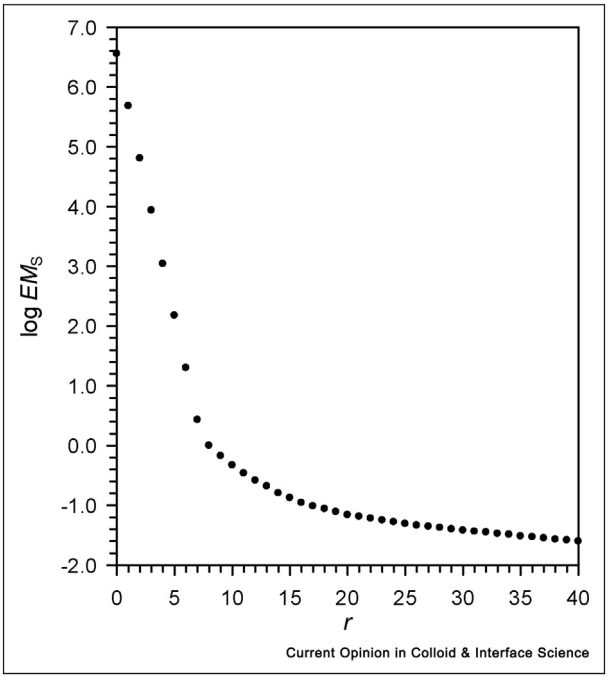

Entropic contribution EM_S (expressed in logarithmic units) to total EM as a function of the number of rotatable bonds r in the linear precursor undergoing a cyclization reaction. Such value coincides with the theoretical value of the EM in the absence of any strain developed in the cyclic transition state ($EM_H = 1$, see Refs. [4,5,7–10] for details).

In addition, driving the cyclization towards the formation of a single stereoisomeric ring when multiple possible isomers can be formed is rather difficult. The higher the number of rings closed in a single process, the harder this problem becomes. A prototypical example is the (poly)cyclization of squalene epoxide to steroids. In bulk solution, this reaction typically affords an intractable mixture of different isomeric cyclized compounds and is synthetically not attractive. In stark contrast, in nature, this reaction occurs inside the well-designed cavity of cyclase enzymes that pre-organizes the substrate and facilitates the reaction, yielding a single stereoisomeric product in high yields [12–14].

In this context, nano-confinement may offer some contributions to address a number of these issues.

First, it can facilitate the cyclization of medium and large rings, a longstanding problem in organic synthesis [7,11]. Preorganization of the linear precursor within the restricted space of a molecule-sized reactor can increase the reaction efficiency in terms of rate and, consequently, yields and selectivities. Preorganization indeed brings the two reactive functions in proximity, exploiting the binding energy of pre-complexation to freeze some rotors in advance.

Second, nano-confinement can offer new opportunities to control the rate, efficiency and selectivity of ring-closure reactions of common cycles. In particular, nano-confinement can drive a linear precursor onto a specific reaction path leading to a single cyclic product, making a strong selection among the several accessible pathways in bulk solution and, ideally, mimicking the selectivity of natural cyclase enzymes [12–14].

The following sections will be classified in consideration of the advantages offered by nano-confinement to tackle some of the open questions in the field.

Cyclization of common rings under nanoconfinement

Confined space catalysis can be efficiently exploited to accelerate cyclization reactions of common rings and hence control their selectivity, favoring the formation of a specific product among the multiple isomers accessible in bulk solution.

In 2008 Rebek's group showed that resorcinarene-based cavitand-acid **1** can selectively catalyze the cyclization of 1,5-epoxyalcohols to 5-membered tetrahydrofuran rings (THF derivative, Figure 2) in mesitylene-d_{12} [15]. 1,5-epoxyalcohol **S1** undergoes acid-catalyzed epoxide ring opening and cyclization to give either a five-member ring (THF product) via 5-exo cyclization, or a six-member ring (tetrahydropyran THP product) via a 6-endo cyclization (Figure 2). Cyclization of **S1** in bulk solution with camphorsulfonic acid furnished THF and THP products **P1a** and **P1b** in a ratio of 87:13. In contrast, confinement of the reaction inside cavitand **1** afforded the THF ring **P1a** as the exclusive product. The cavitands used by Rebek are bowl-shaped resorcinarene-based receptors with a hydrophobic pocket able to host small guests, whose vase-like conformation is maintained by means of a hydrogen bonds network among the amidic functions in the upper rim [16]. In particular, cavitand **1** is endowed with a carboxylic acid moiety that points inside the cavity, well placed to interact with an encapsulated guest and trigger the cyclization. The cavity is key for reactivity, as evidenced by the >50-fold rate acceleration provided by cavitand **1** compared to a model carboxylic acid devoid of the cavity (compound **2**, Figure 2). The catalytic activity of **1** is influenced by the structure of both reactants and products. For instance, the absence of the hydroxyl function in the substrate makes the cavitand unable to bind it, suggesting that the acidic function of **1** serves both for substrate binding and for epoxide activation. There is no product inhibition, but surprisingly the reaction rate decreases on increasing substrate concentration [17]. This is attributed to an interference of the substrates' hydroxyl groups with the hydrogen bonds network at the upper rim of the cavitand, which causes the loss of the vase-like conformation. Analogously, a solvent change from mesitylene to dichloromethane likely reduces the strength of such hydrogen bond network and deactivates the catalyst.

Few years later, the groups of Toste, Bergman and Raymond reported an 8-fold improved activity of a Me_3PAuX (X = Cl or Br) catalyst in the cyclization of an allene-containing alcohol when encapsulated inside coordination cage **3** (Figure 3a) [18]. The increase of hydroalkoxylation activity is provided by the encapsulation which separates the counter anion X^- from the Au(I) complex, generating a more electrophilic and active metal centre, and protects the catalyst from oxidation. Host **3** is a polyanionic tetrahedral cluster $[Ga_4L_4]^{12-}$ (Figure 3a) that encapsulates cationic guests of complementary size, such as complex Me_3PAu^+. The counter anion of the gold complex affects **S2** hydroalkoxylation, with Me_3PAuCl being less efficient than Me_3PAuBr complex (60% and 11% yields, respectively, after 18 h, because of the strongest Au−Br bond). In the case of Me_3PAuBr, an 8-fold rate acceleration is observed within cage **3**, with a 48% yield after 18 h compared to 11% conversion in bulk solution. Encapsulation prevents oxidation and subsequent deactivation of the gold complex, allowing full conversion of the starting allene over 6 days (4.8:1 **P2a**:**P2b** ratio).

Figure 2

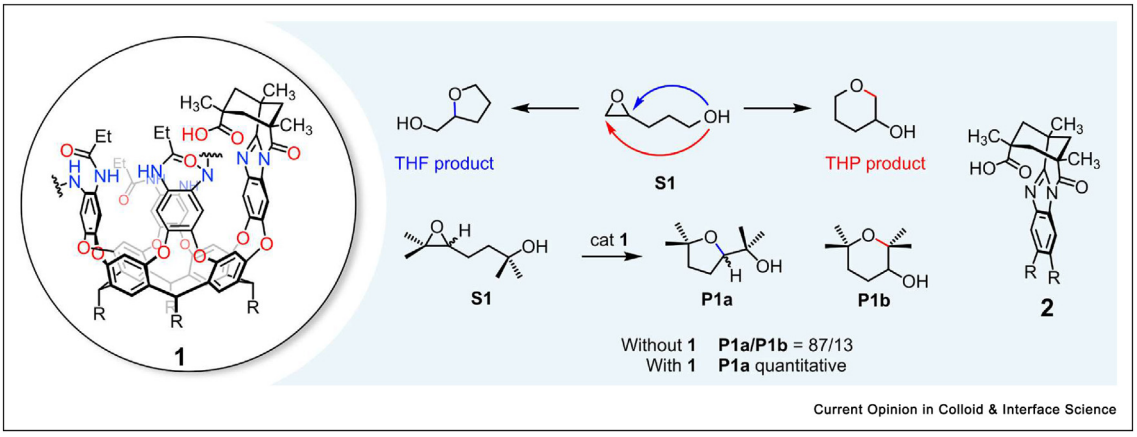

Epoxide ring opening and cyclization catalyzed by cavitand **1** and model **2.**

Figure 3

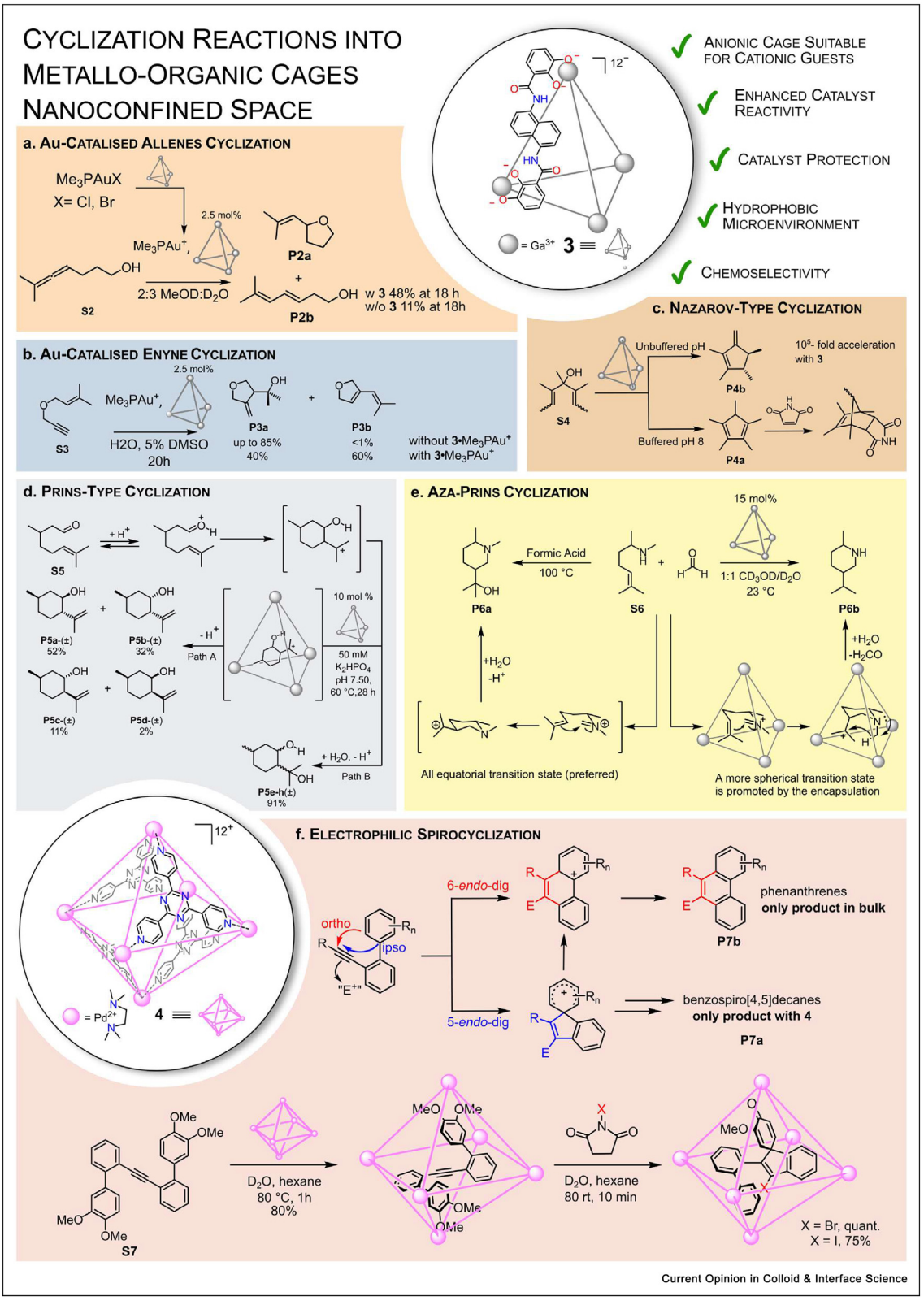

(a) Hydroalkoxylation catalyzed by a gold (I) complex encapsulated in cage **3**. (b) Product distributions for the gold-catalyzed enyne cyclization reactions carried out with or without cage **3**. (c) Different selectivity for the Nazarov cyclization of pentadienols catalyzed by **3** at pH = 8 or at unbuffered pH. (d) Acid-induced (±) citronellal **S5** cyclization: possible paths and product distribution with or without cage **3**. (e) Product selectivity for aza-Prins reactions with or without cage **3**. (f) Divergent electrophile-mediated cyclization of 2-biphenylacetylenes **S7** inside or outside molecular cage **4**.

Similar observations are also made in a related gold-catalyzed enyne cyclization. In bulk solution, using Me_3PAu^+ as catalyst, cyclization of enyne **S3** affords tertiary alcohol **P3a** as the main product. Instead, a 1:1.5 mixture of **P3a** and alkene **P3b** is found for the same reaction performed with the $[Ga_4L_4]^{12-}$ encapsulated gold catalyst (Figure 3b), indicating that nanoconfinement can alter the innate selectivity of the reaction [19].

The same groups used the $[Ga_4L_4]^{12-}$ tetrahedral cage **3** to catalyze the Nazarov cyclization of bisallylic alcohol **S4** to **P4a** with a stunning million-fold rate enhancement compared to the uncatalyzed reaction (Figure 3c) [20,21]. Such Nazarov cyclization usually requires acidic conditions to generate the carbocationic intermediate that undergoes rate-determining electrocyclization. Inside the cavity, the carbocation is stabilized by cation-π interactions with the electron-rich aromatic walls and by electrostatic interactions with the twelve negative charges of **3**, and pre-organized for the cyclization. Therefore, in the cage-catalyzed cyclization, the loss of water and the ring closure have comparable rates, much higher than in bulk solution [20]. Competitive encapsulation of product **P4a** causes a strong product inhibition, which can be avoided by adding maleimide as a product scavenger (Figure 3c). In the latter case, the reaction continues until full substrate conversion. If the water solution is buffered (pH = 8), cyclopentadiene **P4a** is the only product formed, while in unbuffered D_2O the reaction yields dihydrofulvene **P4b** as a product, due to a kinetically controlled regioselective deprotonation of the cationic intermediate within the capsule. In contrast, no regioselectivity is found for the reaction carried out in the absence of the capsule.

In 2012 cage **3** was used to catalyze the Prins-type cyclization of monoterpene (±) citronellal **S5** at physiological pH and moderate temperature into a set of different cyclic terpene species, different from those observed in bulk solution (Figure 3d) [19]. The cyclization yields a similar carbocationic intermediate which can evolve following two divergent paths: the first (unfavored) one affords diastereoisomeric products **P5a-d**, while the second (favored) one leads to a mixture of four diastereoisomeric *p*-menthane-3,8-diols **P5e-h**. Thanks to its twelve negative charges and electron-rich aromatic walls, cage **3** stabilizes the cationic intermediates involved in citronellal cyclization, facilitating the reaction, and furnishes a mixture of pulegol derivatives **P5a-d** in 97% yield under mild conditions (pH 7.5, 60 °C). The alkene is formed because the hydrophobicity of the cavity of cage **3** provides a water-free microenvironment, where elimination of the carbocation is preferred over its hydration. In contrast, in bulk solution at pH 3.2 (KH_2PO_4 catalyst, 50 °C, 8 h), cyclization yields diols **P5e-h** as main products (91%) accompanied by low amounts of **P5a-d** (9%).

Cage **3** can also catalyze other reactions involving cationic intermediates, such as aza-Prins cyclization, with an unnatural selectivity (Figure 3e) [22]. Heating a mixture of amine **S6** and formaldehyde in the presence of formic acid induces an aza-Prins cyclization to product **P6a**. In the presence of 15% **3** at 23 °C, product **P6b** was found instead, with a remarkable change in reaction mechanism. After formation of the iminium ion and ring closure (Prins cyclization), a 1,5-hydride shift occurs inside the confined space, followed by facile hydrolysis of the resulting iminium ion to piperidine **P6b**. Such divergence in product selectivity is rationalized by taking into account the different conformations of the cationic intermediate (and the related six-membered, cyclic transitions state) that undergoes cyclization. In bulk solution, all substituents are in equatorial positions, and the carbocation is too far away for an intramolecular hydride shift. Encapsulation within the $[Ga_4L_4]^{12-}$ cage favors a more spherical conformation where the isopropyl cation is in the axial position, and a 1,5-hydride shift from the *N*-methyl group becomes feasible.

In 2022 Takezawa, Fujita and co-workers reported that molecular hollow-cage **4** (Figure 3f) can invert the selectivity of the electrophile-mediated cyclization of 2-biphenylacetylene **S7** in water [23]. In bulk solution, **S7** undergoes the expected cyclization from the *ortho* carbon to give phenantrene **P7b** (6-endo-dig cyclization, quantitative yield). Cage **4** is an octahedral host self-assembled from palladium salts and a tritopic ligand that encapsulates **S7** in a bent conformation in which the *ipso* carbon is close to the acetylene carbon, as confirmed by ^{1}H-NMR and X-Ray diffraction data. Subsequent treatment of the adduct with 1.1 molar equivalents of *N*-halosuccinimide yields an elusive benzospiro [4,5]decane **P7a** via unfavorable 5-endo-dig cyclization (quantitative yield with of *N*-bromo succinimide, 75% with N-iodo succinimide, Figure 3f).

Tiefenbacher's group explored the selective cyclization of different linear monoterpenes in chloroform catalyzed by 10 mol% supramolecular capsule **5** (Figure 4a) [24]. Capsule **5** is obtained by the self-assembly of six molecules of resorcinarene **6** and 8 to 15 water molecules in apolar solvents and has an internal cavity with a volume of ∼1400 Å^3. It is slightly acidic (p*Ka* ≈ 5.5−6) thanks to charge dispersion over the extended hydrogen bond network [25] and is able to stabilize encapsulated cationic species by means of cation-π interactions with its electron-rich aromatic walls. Moreover, it acts synergistically with HCl co-catalyst (up to 10 mol%) in the generation of reactive carbocationic intermediates [26,27]. Capsule **5** (10 mol%) can mimic natural cyclase enzymes catalyzing the cyclization of geraniol, linalool and nerol or the corresponding acetates to cyclic products such as eucalyptol or terpinene. In the presence of **5**, the reaction occurs via an elusive tail-to-head cationic cascade cyclization which can stop at the first cycle (i.e.

Figure 4

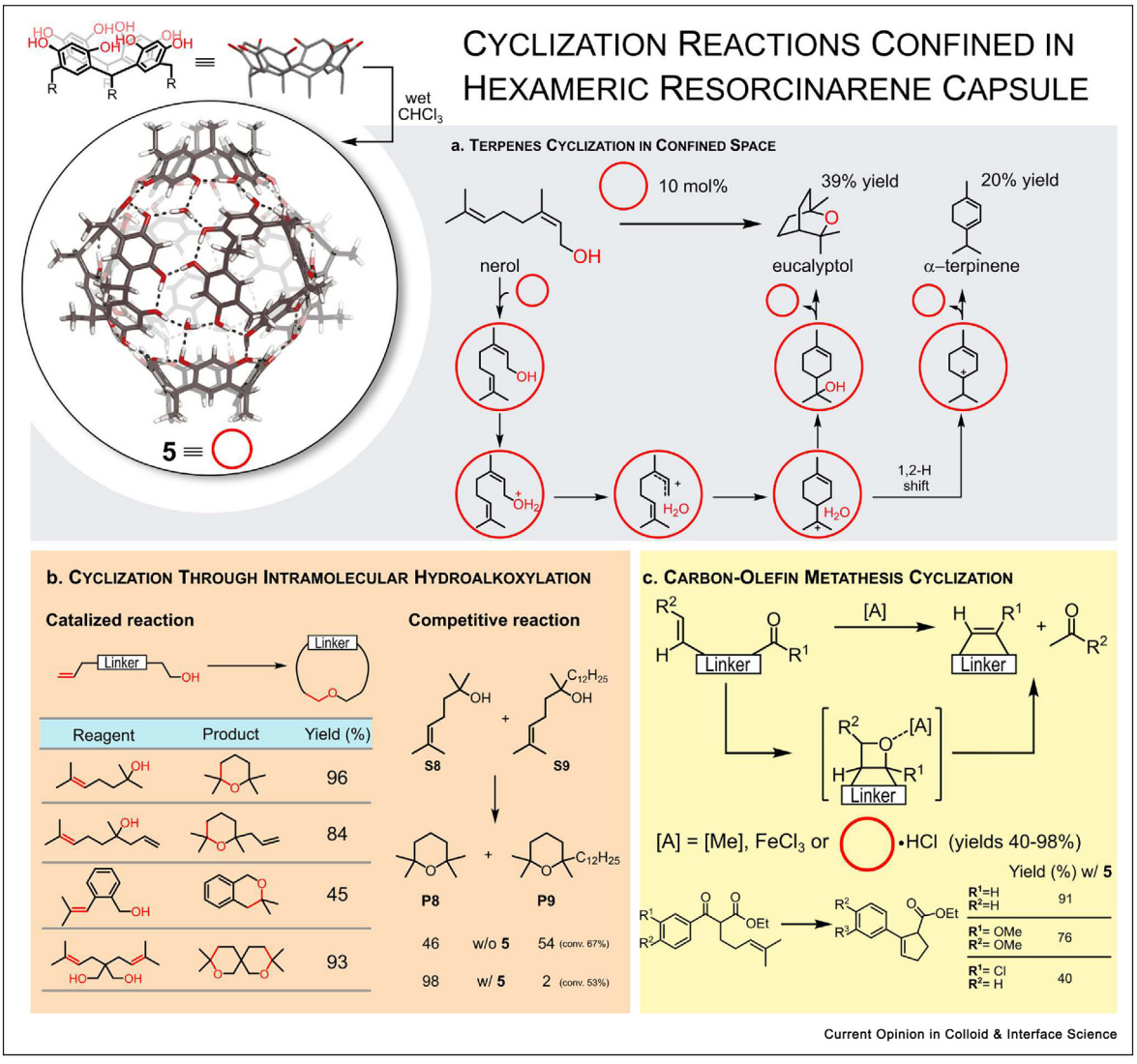

a) Terpene cyclization: possible paths and cyclization inside capsule **5**. b) Intramolecular hydroxyalkylation of unsaturated alcohols inside capsule **5**. c) Carbonyl-olefin metathesis catalyzed by stoichiometric or catalytic amounts of Lewis acid or by a catalytic amount of **5** and HCl.

α-terpinene) or yield more complex bicyclic structures (i.e. eucalyptol). If the capsule is absent or occupied by $Bu_4N^+Br^-$ (which displaces the substrates from the cavity), no cyclization is observed. The cavity stabilizes and shields from nucleophilic quenching the carbocation intermediates, which can undergo ring closures or isomerizations (Figure 4a).

The same group also reported that capsule **5** catalyzes the intramolecular hydroalkoxylations of unsaturated alcohols to 6- and 7-membered ring ethers or spirobicyclic rings under mild conditions and good to high yields (45–98%, Figure 4a) [28]. In bulk solution, such cyclizations require strong acids [29], which, however, tend to induce unwanted side reactions that reduce selectivity. Inside the capsule, the reaction takes place under mild conditions (chloroform, 30 °C, 10 mol% **5**) and higher selectivity. Again, in the presence of $Bu_4N^+Br^-$, which irreversibly enters inside the capsule acting as an inhibitor, only a background conversion is observed. Furthermore, the limited volume of the resorcinarene capsule imposes a high size selectivity. When the competitive cyclization of substrate **S8** and its larger analogue **S9** is carried out in bulk in the presence of 10% of triflic acid, there is no substrate selectivity (**P8**/**P9** = 46:54). In contrast, in the presence of 10% **5** the **P8**/**P9** product ratio is 92:8, because the smaller **S8** fits better inside the capsule cavity where the reaction occurs (Figure 4b).

Resorcinarene capsule **5** and HCl can also act synergistically to achieve ring-closing carbonyl-olefin metathesis (Figure 4c) [30]. Carbonyl-olefin metathesis forms a new C=C bonds from an alkene and a ketone or an aldehyde under strong Lewis acid catalysis and can be used for ring closures. However, reaction conditions are usually harsh and require transition metal catalysts ($FeCl_3$), often in stoichiometric amount. Capsule **5** (10 mol%) and HCl (5 mol%) co-catalyze carbonyl-olefin metathesis in chloroform at 50 °C, with yields ranging from 40% to 98%. Keys to such reactivity are the strong acidity of the **5**-HCl system, the stabilization of the cationic intermediates, and substrate pre-organization upon encapsulation. Again, the reaction is size-selective when occurring inside the cavity.

Cascade cyclizations

Nanoconfinement can be also used to achieve selective cationic cascade reactions in which elusive strained and/or complex polycyclic systems are obtained. The confined environment indeed shields the cationic intermediates from a premature nucleophilic quenching, unlocking reaction paths unavailable in bulk solution.

Capsule **5** (10 mol%) converts unsaturated alcohols into bicyclic alkenes via cationic cascade reactions (cyclodehydration and rearrangements) within the cavity under mild conditions (chloroform, 50 °C, Figure 5a) [31]. The reaction mechanism involves the formation of an α-spirocyclic carbocation from substrate **S10** followed by (i) a 1,2 hydride shift and (ii) a final rearrangement to afford product **P10**. In the presence of inhibitor $Bu_4N^+Br^-$ or without the cage (trifluoroacetic acid is used as a catalyst), the products are obtained in poor yields and no substrate selectivity.

Capsule **5** and HCl can act synergistically as cyclase mimics in the cyclization of sesquiterpenes to bicyclic and tricyclic compounds under mild conditions (10 mol% **5** and 3 mol% HCl, chloroform, 30 °C, Figure 5b) [32,33]. The cyclization of linear sesquiterpenes occurs smoothly on several isomers of farnesol **S11(OH)** and farnesyl acetate **S11(OAc)** differing for the C=C bond geometry (2*Z*,6E, 2*Z*,6*Z* and 2E,6*Z*). Different polycyclic products can be obtained, such as 2-epi-α-cedrene, α-cedrene, ϵ-patchoulene, δ-selinene and 10-epi-zonarene. For both alcohols and acetates, the best product selectivity is found for the (2E, 6*Z*) isomers, with the main products being δ-selinene **P11a** and 10-epi-zonarene **P11b** (0–22% yield and 4–12% yield, respectively, depending on reaction conditions and C=C bond geometry of the substrates). The route to δ-selinene starts with a 1,10-cyclization (Figure 5b) forming a rigid cyclodecadiene cation as a first intermediate, which evolves through a cationic reaction cascade. Using monocyclic sesquiterpenes such as cyclofarnesyl acetates **S12** (*Z* and E) as substrates, the main product is tricyclic isolongifolene **P12** with an isolated yield of 11% (Figure 5c). In fact, this is the shortest artificial synthesis reported so far for isolongifolene **P12** (four synthetic steps only from commercial dihydro-β-ionone). Cyclization of cyclofarnesyl derivatives is reported in literature to occur in bulk solution using chlorosulfonic acid as a catalyst, but three different products are formed as a result of the reaction cascade, and isolongifolene is not among them [34].

Capsule **5**-catalyzed cyclization also enables the synthesis of other complex natural products, such as (−)-Presilphiperfolan-1β-ol **P13**, even in preparative scale under mild conditions (Figure 5d) [35]. The starting material is alcohol **S13**, which is obtained in three steps from (−)-caryophyllene oxide. Then, **5** catalyzed cyclization furnishes **P13** in 35% yield (26.6% overall yield). Use of the synthetic capsule **5** instead of a natural enzyme allows the synthesis of several unnatural cyclic C-4 substituted derivatives of **P13**.

Enantioselective cyclizations

Carrying out a reaction within a confined molecular-sized space can largely affect the stereoselectivity of the reaction with the preferential formation of one specific isomer over the others. In fact, if the environment inside the confined space is asymmetric, chirality can be transferred to the reaction products.

Natural cyclodextrins are water soluble, cyclic oligosaccharides composed of D-(+)-glucopyranose monomer units, characterized by a hydrophobic and chiral cavity that can host lipophilic guests, where the hydrophobicity is imparted by aliphatic C–H bonds. In a series of seminal works, Sollogoub and coworkers designed cyclodextrins endowed with different transition metal complexes whose catalytically active sites point inside the cavity. Such structures are particularly suited to catalyze chemical reactions, mimicking the operation of metalloenzymes. The metal ion is forced to be buried inside the hydrophobic cavity by a rigid, well-oriented *N*-heterocyclic carbene (NHC) ligand, which binds an Au(I) metal cation competent for enyne cyclizations [36]. As shown below, factors such as the size of the cyclodextrin cavity, the solvent used or the dimension of the reactants, can affect the reaction outcome in terms of yield, enantiomeric excess or products distribution.

The two gold–cyclodextrins complexes **6α·AuCl** and **6β·AuCl** (Figure 6a) were used as precatalysts for the stereoselective cyclization of *N*-tethered 1,6-enyne **S14** to **P14** and compared with the carbene complex IPr·AuCl model (chloro-[1,3-bis(2,6-diisopopylphenyl)imidazo-2-ylidene gold (I)) [37]. The gold-complex precatalyst needs to be activated by addition of a silver salt, which abstracts the chloride ion and unmasks the Au^+ cation. In the case of the model catalyst IPr·AuCl, no asymmetric induction is observed, as expected (80% yield, 0% ee, see

Figure 5

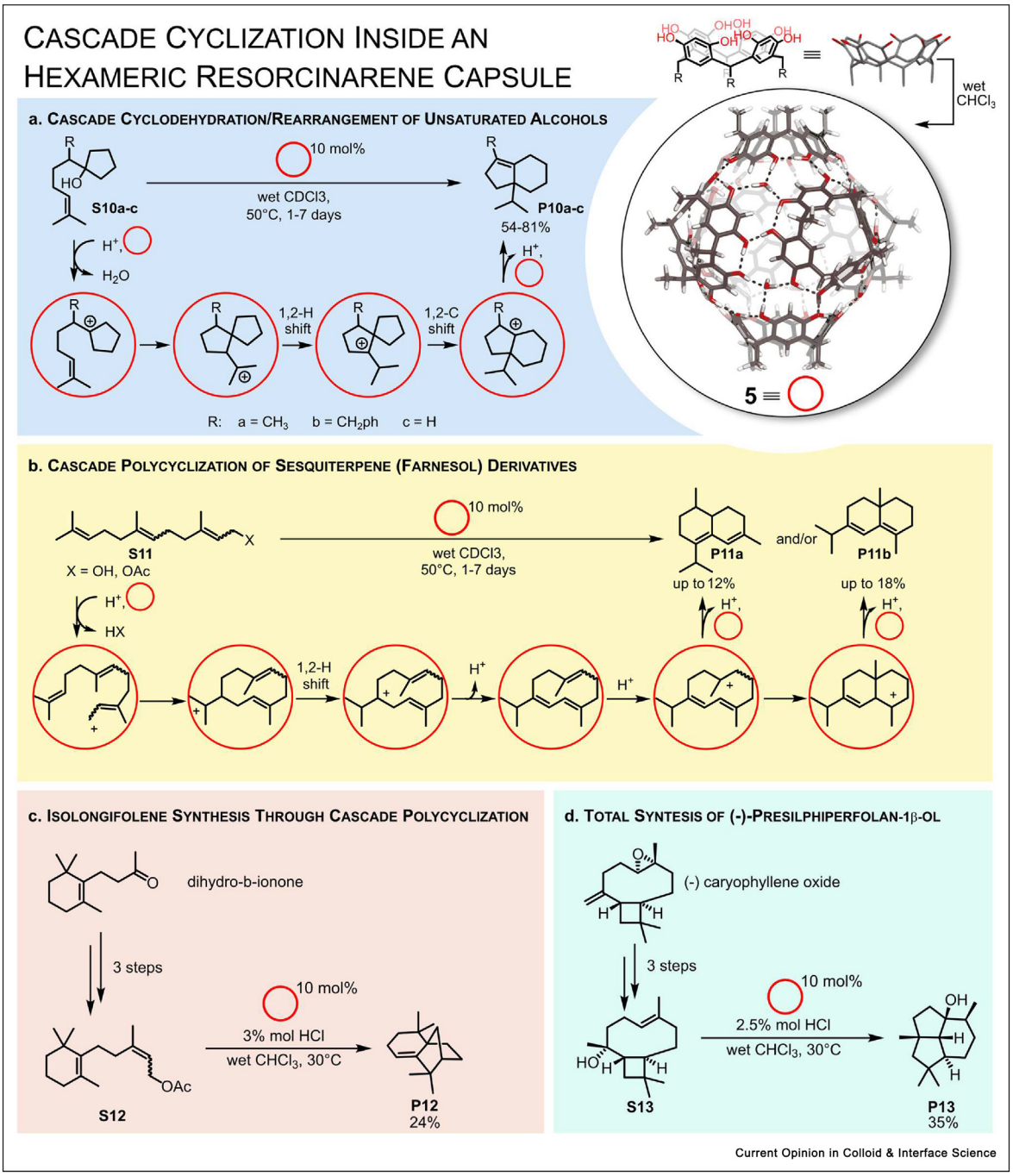

Representative examples and related product yields for **5** catalyzed cascade cyclizations: (a) cascade hydroalkoxylation/rearrangement. (b) Cascade cyclodehydration of sesquiterpene farnesol derivatives **S11**. (c) Cascade cyclization of a cyclofarnesyl derivatives applied to a concise synthesis of Isolongifolene. (d) Short total synthesis of (–)-presilphiperfolan-1β-ol **P13** and unnatural derivatives via a cascade cyclization.

Figure 6a). When catalysts **6α·AuCl** and **6β·AuCl** are used, the reaction occurs with a modest, yet promising, enantioselectivity (43 and 59% *ee*, respectively) and good yields (83 and 77%, respectively), demonstrating that chirality induction from cyclodextrins cavities is possible. Subsequently, different stereoselective cycloisomerizations of 1,6-enynes and N-tethered enynes with gold-cyclodextrin catalysts based on different NHCs-ligands and including the γ-cyclodextrin moiety have been also explored [38].

Figure 6

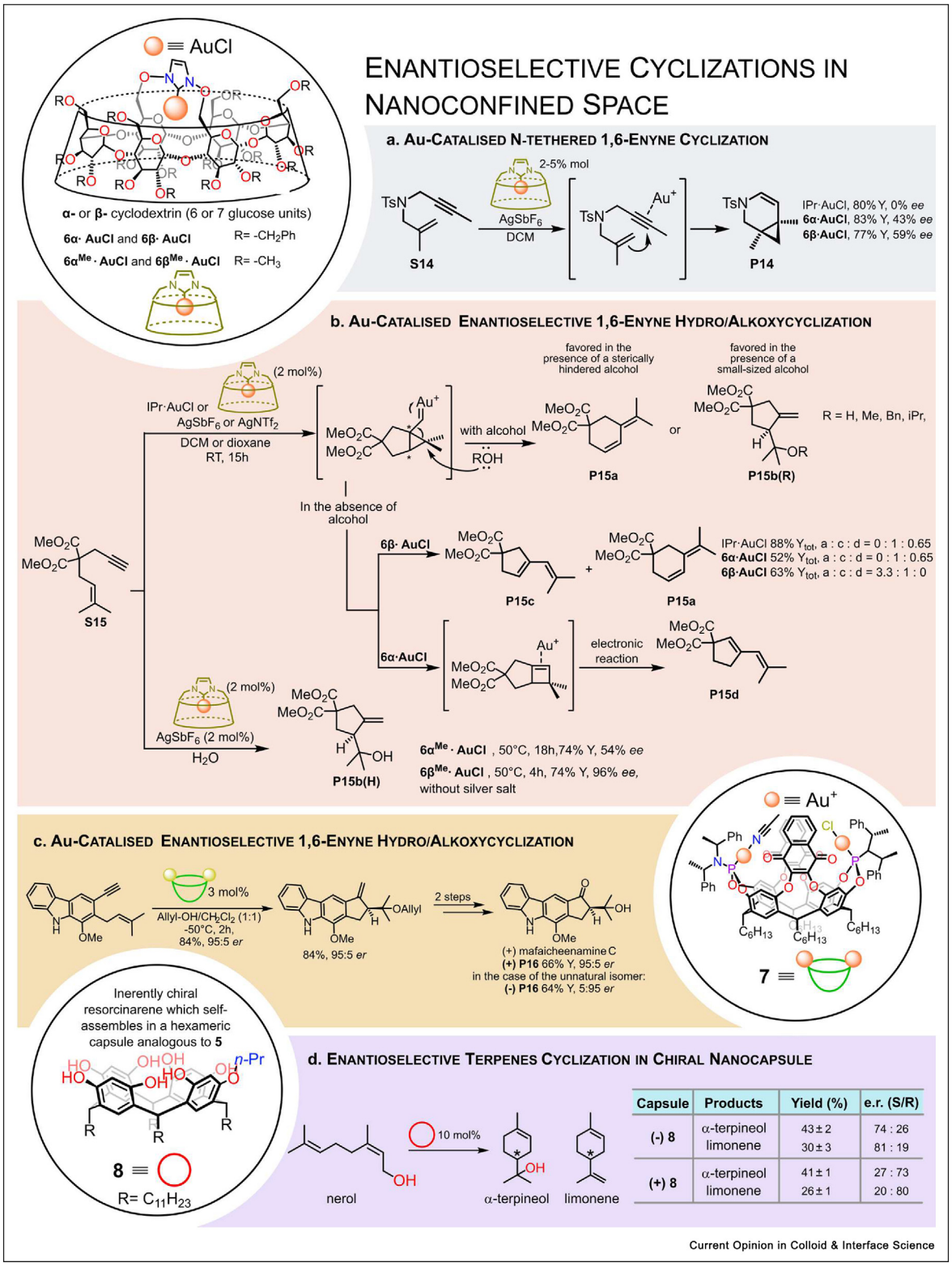

(a) Stereoselctive cyclization of 1,6*N*-tethered enyne **S14** catalyzed by the Au (I) cyclodextrin complexes **6α·AuCl** and **6β·AuCl**. (b) Alteration of selectivity in the **6α·AuCl** and **6β·AuCl** catalyzed cyclization of 1,6-enyne **S15**. (c) Asymmetric 1,6 enyne alkoxy- or hydro-cyclization catalyzed by **6α·AuCl** and **6β·AuCl** in the presence of ROH nucleophiles and by **6α^{Me}·AuCl** and **6β^{Me}·AuCl** in water. (d) Concise total synthesis of (+)-mafaicheenamine C with an asymmetric enyne cyclization catalyzed by cavitand-based Au catalyst **7**. (e) Asymmetric cyclization of nerol catalyzed by the inherently chiral self-assembled resorcinarene cage **8**.

Precatalyst **6β·AuCl** can also perform highly enantioselective alkoxycyclization of 1,6-enynes such as **S15**. When a small-sized alcohol is present, the 5-membered ring product **P15b(R)** is formed via nucleophilic attack of the alcohol on the reaction intermediate (Figure 6b, top) [39]. Conversely, if the alcohol is sterically hindered (such as isopropanol), the limited size of the cavity hosting the cationic intermediate disfavors its addition and the reaction evolves to **P15a**. In the absence of any nucleophile, the reaction proceeds favoring the formation of the six-membered ring **P15a** instead of the five-membered one. Under the same conditions, pre-catalysts **6α·AuCl** and IPr·AuCl favor the formation of the five-membered ring **P15d** (compare **P15a,c,d** ratios reported in Figure 6b, middle) [37]. In water environment, the more soluble methyl-derivatives **6α^{Me}·AuCl** and **6β^{Me}·AuCl** (with improved solubility) catalyze a similar enantioselective hydroxycyclization of 1,6-enyne **S15** to cyclic tertiary alcohol **P15d(H)**, where the water acts as the nucleophile that quenches the cationic intermediate (see Figure 6b, bottom) [40]. The reaction does not need the silver salt additive, and the best results are indeed achieved in the presence of **6β^{Me}·AuCl** without silver salt (74% yield, 96% *ee*, 4 h). Probably, in aqueous environment, the substrate is forced to reside within the hydrophobic cavity improving the efficiency of the chirality transfer. Other cyclization reactions such as lactonizations and regioselective hydroarylations were also explored [40].

Several research groups designed Au (I) catalysts buried within basket-shaped molecules such as calixarenes [41] and resorcinarenes [42–44]. In particular, Echavarren's group reported a chiral resorcinarene-based cavitand gold (I) complex that catalyzes a highly enantioselective alkoxycyclization of 1,6-enynes (Figure 6c) [45]. Among the different cavitand-based catalysts investigated, the best results are afforded by bimetallic complex **7** (Figure 6c). This catalyst enables the asymmetric alkoxycyclization of 1,6-enynes that can be used as key enantiodetermining step in the total synthesis of both enantiomers of mafaicheenamine C **(±)-P16** with the opposite cavitand enantiomers (66% yield and 95:5 er for the natural (+) isomer, while the unnatural (−) isomer was obtained in 64% yield and 5:95 er).

In 2022 Tiefenbacher's group reported that an inherently chiral analogue of resorcinarene capsule **5** can be used to achieve enantioselective cationic terpene cyclization reactions (Figure 6d) [46]. As previously discussed, **5** is able to catalyze the tail-to-head cyclization of terpenes with small amounts of HCl as cocatalyst in chloroform under mild conditions [47]. Several chiral homologous of the capsule were studied, among which capsule **8,** obtained by the self-assembly of six molecules of a chiral resorcinarene and eight water molecules, emerged as the best chiral catalyst. In the **5**-catalyzed cyclization of nerol, four different products are obtained: chiral α-terpineol, limonene, achiral eucalyptol and α-terpinene. Using chiral catalyst **8** as a catalyst for the cyclization, enantioenriched products (up to 81:19 *e.r.*) were obtained, mimicking the chiral pocket of natural cyclase enzymes.

Macrocyclizations

As stated before, macrocyclizations are challenging reactions because of the low value of EM associated with the closure of large rings. This low value of EM is mainly due to the large conformational space that the long-chain precursors can explore. In the case of medium rings (8–11 membered rings) the problem can be additionally complicated by the insurgence of high-strain energy at transition state level (due to Prelog transannular interaction, *vide supra*). Confining a long-chain molecule inside a molecular host diminishes the conformational freedom of the linear precursor, favoring its cyclization. Moreover, the interactions between the cavity and the guest may catalyze the reaction by selectively stabilizing the transition state and, consequently, lowering the overall kinetic barrier.

In the following section, some examples of molecular vessels used to promote macrocyclization reactions are summarized. Rebek and coworkers pioneered the field using a series of structurally similar cavitands (see Figure 7) in stoichiometric or super-stoichiometric amounts to favor the macrocyclization of α,ω-difunctionalized substrates.

In 2015, they took advantage of cavitand **9a** to promote the formation of large 12- and 13-membered lactams starting from the corresponding α,ω-amino acids (C11 and C12, respectively) [48]. Cavitand **9a** is water soluble due to the presence of ionic groups in its backbone (see Figure 7) and binds both ω-aminoundecanoic and ω-aminododecanoic acids. Both guests tend to assume a U-shaped conformation inside the cavitand, with the middle portion of the chain deeply buried inside the hydrophobic cavity and the terminal polar functionalities exposed to the solvent and held in close proximity. To achieve the cyclization, the authors treat a water solution containing an excess of cavitand **9a**, substrate, EDC (1-ethyl-3-(3-dimethylamino)propyl carbodiimide) and sulfo-NHS (sulfo-N-hydroxy-succinimide). Cavitand **9a** improves product yield by a factor of 4.1 and 2.8 in the formation of the 12-membered and 13-membered lactam, respectively, compared to bulk solution. In both cases, in the absence of cavitand **9a** mostly oligomeric products are detected.

In 2016 the same group exploited cavitand **10b** to promote the macrocyclization of a series α,ω-diisocyanates (from C9 to C12) to form macrocyclic ureas (12- to 15-membered ureas) (see Figure 7b) [49]. Again, mixing of substrate and cavitand **10b** in water yields the corresponding stoichiometric complex. Inside cavitand **10b**,

Figure 7

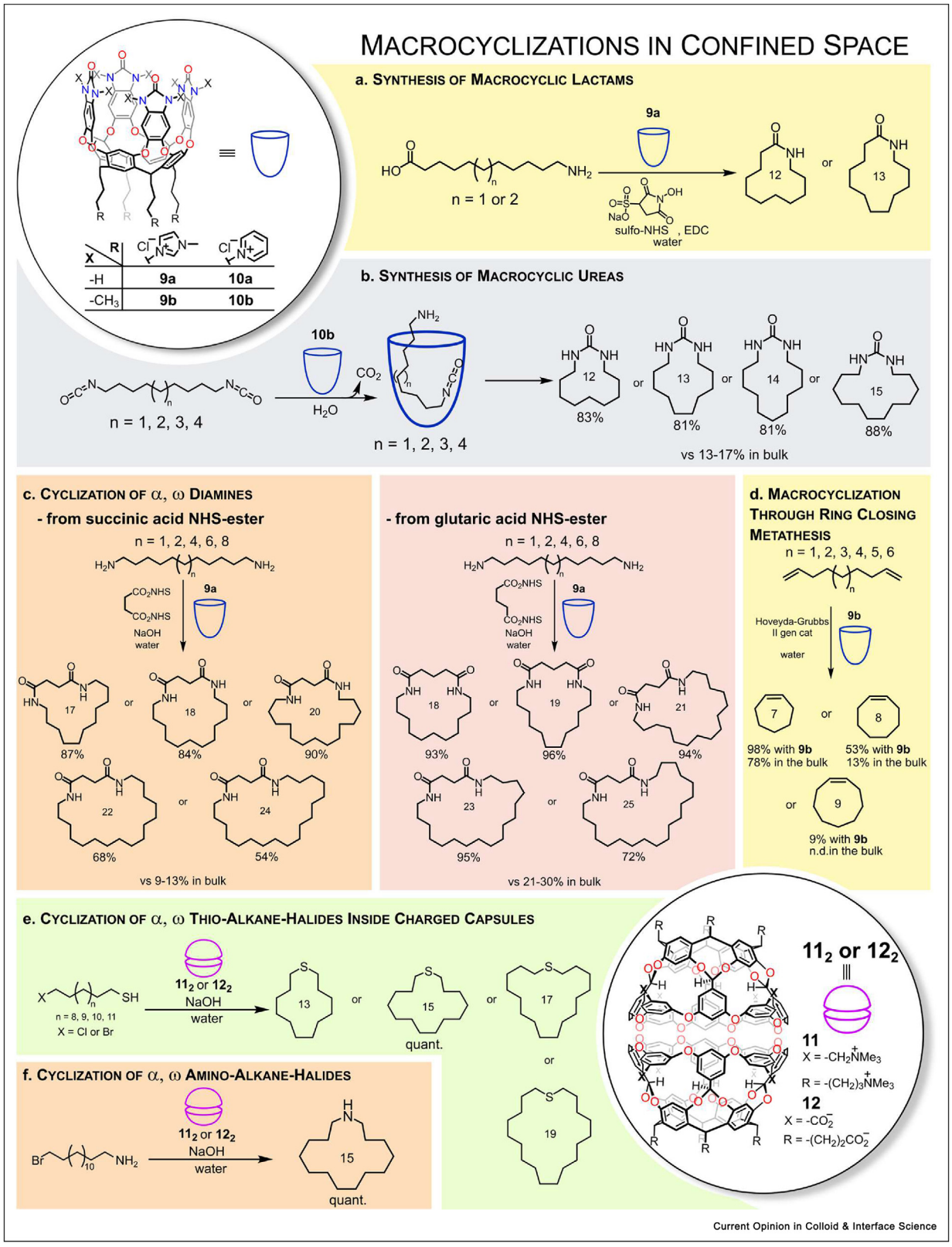

(a) Macrolactamization of α,ω aminoacids promoted by cavitand **9a**. (b) Formation of macrocyclic ureas. (c) Macrocylization of α,ω diamines. (d) Macrocyclization via ring-closing metathesis. (e) Macrocyclization of α,ω thiohalides inside capsule $\mathbf{11_2}$ or $\mathbf{12_2}$. (f) Macrocyclization of α,ω aminohalides.

Figure 8

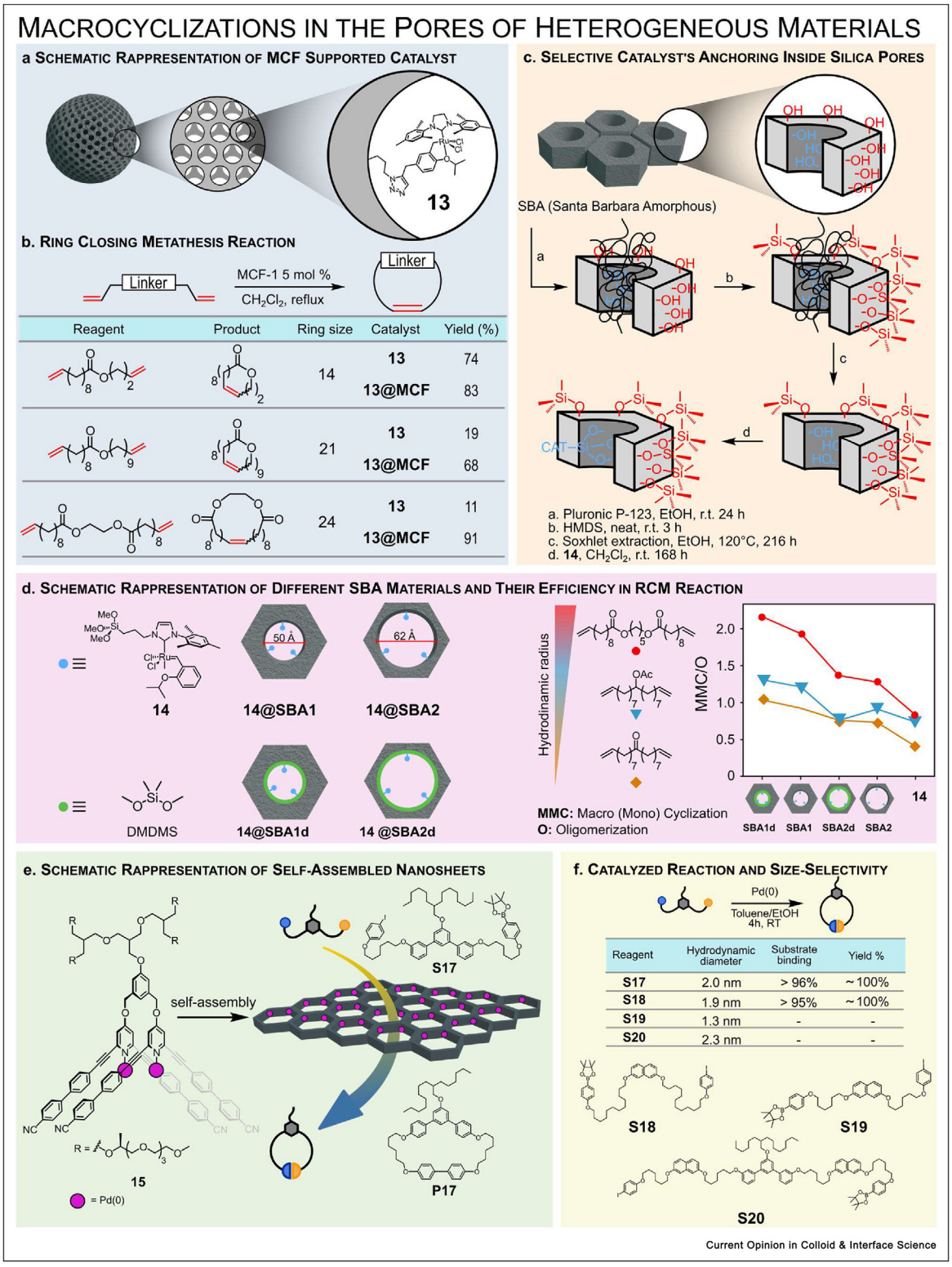

(a) Schematic representation of the morphology of mesocellular siliceous foam (MCF), highlighting the anchored Hoveyda-Grubbs type catalyst **13**. (b) RCM catalyzed by catalyst **13** and **13**@MCF. (c) Schematic representation of the synthesis and morphology of **SBA1** and **SBA2**. (d) Schematic representation of **14**-loaded SBA materials and related MMC/O ratios obtained in RCM. (e) Representation of the morphology of self-assembled porous nanosheets. (f) Suzuki–Miyaura macrocyclization of substrates with different hydrodynamic diameters.

the α,ω-diisocyanate substrate assumes a bent conformation, with one of the isocyanate groups buried inside the cavitand and protected from the solvent. In contrast, the other isocyanate group is exposed to water and reacts with it, producing a carbamic acid, which rapidly loses CO_2 to give the final amine-monoisocyanate. Inside the cavitand, the highly nucleophilic amino group quickly reacts with the isocyanate function to form a macrocyclic urea. In the presence of cavitand **10b**, the yields for the macrocyclic ureas are 81−88% and intermolecular reactions to form oligomers are inhibited, while in its absence the yields dropped to 13−17% (10% acetone is used as a cosolvent to solubilize the substrates; in its absence, no macrocyclic ureas are detected).

Cavitand **9a** can also promote the macrocyclization of α,ω-diamines (namely C11, C12, C14, C16 and C18) in water by reaction with succinic anhydride and EDC/NHS or succinic and glutaric NHS-esters (see Figure 7c) [50]. Again, substrates and **9a** give the 1:1 corresponding complex where the included substrates assume U-shaped conformations exposing the two amino groups to the water and forcing them to be in proximity. Reaction of these adducts with succinic anhydride in the presence of NaOH produces clean monoacylated products, namely α,ω-amino acids. Then, addition of EDC and NHS affords the corresponding macrocyclic dilactams in 66 and 64% yield in the case of C11 and C12 diamines, respectively. Direct macrocyclization of α,ω-diamines to the corresponding dilactams is achieved by using NHS-ester of succinic or glutaric acid and NaOH. In the case of succinic acid, macrocyclization yields span from 84 to 90% for C11, C12 and C14 α,ω-diamines, 68% for C16, and 54% for C18, to be compared with around 10% yield in the absence of cavitand **9a** (Figure 7c). In the case of glutaric acid NHS ester, the direct macrocyclization of α,ω-diamines affords yields above 90% for C11, C12, C14 and C16 and 72% for C18 α,ω-diamines, to be compared with 20−30% yield in the absence of cavitand.

In 2018, Rebek and coworkers exploited cavitand **9b** to obtain macrocyclic olefines via ring-closing metathesis (RCM) of α,ω-dienes using 3% of Hoveyda-Grubbs II generation catalyst in water [51]. Cavitand **9a** tends to dimerize into a capsule when a large hydrophobic guest is present, but exhaustive *N*-methylation of the benzimidazolones moieties at the upper rim of the molecular vessel prevents the dimerization (cavitand **9b,** see Figure 7d). Thus, in the presence of cavitand **9b** and 3% of Hoveyda-Grubbs II gen catalyst, C9 and C10 α,ω-dienes evolve to the corresponding seven- and eight-membered cyclic olefins with high yields (98% and 53%, respectively) to be compared to 78% and 13%, respectively, in the absence of the cavitand in chloroform solution. With C11 α,ω-diene, only 9% of the corresponding nine-membered cyclic olefin product is detected in the presence of the cavitand **9b,** while no trace of product is found in its absence. In the case of longer α,ω-dienes guests (from C12 to C14), the same macrocyclization reaction with cavitand **9b** is unsuccessful. The same cavitand catalyst **9b** was later applied to an intra(macro)molecular aldol condensation of linear α,ω-dialdehydes to the corresponding condensation macrocyclic unsaturated aldehydes [52]. Also in this case, preorganization of the encapsulated substrate is key for selectivity: in the absence of cavitand the reaction yields mainly oligomeric products (linear and cyclic), while in its presence selective macrocylization occurs efficiently to afford cyclic unsaturated aldehydes in 71−85% isolated yields. Again, chain length affects reaction efficiency (formation of 11-membered cycles does not occur, that 12-membered cycle is slow but accelerates upon increase of cycle size), and substitution of methylene linker with -O- or -S- ones is well tolerated.

Aside from the cavitands, molecular capsules can also provide a confined space to favor macrocyclization reactions in a similar manner. Gibb's group explored the use of supramolecular capsules with chemically identical inner cavities but different charge (+ or −) of the electrostatic potential (EP) that wraps them ($\mathbf{11_2}$, positive, and $\mathbf{12_2}$, negative, see Figure 7e−f). Cavitand precursors **11** and **12** contain a hydrophobic pocket and when a sufficiently large guest is present in solution, two units self-assemble around the guest, giving the adducts $\mathbf{11_2}$ and $\mathbf{12_2}$, respectively. The hydrophobic inner space of these capsules is not uniform, but is more polar at the equatorial region and less polar at the poles due to the different functions present and a heterogeneous distribution of the externally charged functionalities. As stated before [16], long guests tend to assume bent conformations inside capsules $\mathbf{11_2}$ and $\mathbf{12_2}$. Initially, Gibb and coworkers specifically investigated how the charge of the EP can influence the macrocyclization of α,ω-thio-alkane halides (namely C12, C14, C16 and C18) to the corresponding 13-, 15-, 17-, 19-membered thio-ethers inside capsules $\mathbf{11_2}$ and $\mathbf{12_2}$ [53]. The cyclization reactions were carried out by treating a water solution of the 2:1 cavitand−substrate complexes with NaOH. The reaction is quantitative in all cases and follows an apparent first-order kinetic that is affected by i) the nature of the leaving group (brominated substrates always react faster than chlorinated ones), ii) conformation of the substrate inside the capsule, with longer guests reacting faster because of their preorganized J-shaped conformation with the two reactive ends in proximity, and iii) the external charge of the capsule. Specifically for this last point, the macrocyclization occurs thousands of times faster in the positively charged capsule $\mathbf{11_2}$ than in the negatively charged one $\mathbf{12_2}$. Such acceleration is in part due to an increase of S−H function acidity inside the positively charged capsule $\mathbf{11_2}$, especially when located in the equatorial region exposed to water solvent. In fact, titrations with NaOH of long-chain thiols highlight an

enhanced acidity inside the positively charged capsule $\mathbf{11_2}$ compared to the negatively charged one $\mathbf{12_2}$. Moreover, Eyring analysis of selected cyclization reactions inside the two capsules shows that the rate acceleration in $\mathbf{11_2}$ arises from enthalpic effects induced by the electrostatic potential. Entropic factors are similar in both cages, as substrate preorganization is analogous.

In 2021 Gibb and coworkers studied the rate and activation parameters for the cyclization of an α,ω-aminobromoalkane (namely 14-bromotetradecan-1-amine) inside capsules $\mathbf{11_2}$ and $\mathbf{12_2}$, both in the absence and presence of external ions (added as salts) able to attenuate the EP *via* binding to the external charged groups of the capsules [54]. The authors concluded that the capsules act as supramolecular electron withdrawing ($\mathbf{11_2}$) or donating ($\mathbf{12_2}$) groups that, interacting with the electron density of the transition state, induce a deviation from the ideal S_N2 mechanism [55].

An interesting extension of this approach entails the catalysis of macrocyclizations in the confined porous solid supports, mainly mesoporous silica, where appropriate catalysts are immobilized. Even though supported catalysts were initially developed to improve separation, reusability and recyclability, such an approach can also promote entropically unfavored (mono)macrocyclizations over oligomerizations. The advantage offered by such materials resides in their porous morphology, which limits the accessibility of more than one substrate molecule inside the confined catalytic site favoring intramolecular reactions (i.e. cyclizations) over the intermolecular counterpart. Consequently, high macrocyclization yields can be achieved at relatively high substrate concentrations, avoiding diluted conditions. Moreover, the possibility to obtain materials with a precise pore size, which can be further tuned by means of post-functionalization processes, offers unique opportunities to achieve and modulate substrate selectivity.

In 2013, Lee et al. reported a mesocellular siliceous foam (MCF)-supported Hoveyda-Grubbs type catalyst for olefin metathesis (Figure 8a) [56]. MCF is a mesoporous silica material featuring a large surface area resulting from large networked nanopores, which allow facile substrate diffusion into the material (Figure 8a). Catalyst **13**, anchored to the silica walls via a click reaction, proved to be very efficient in RCM. Inside MCF, macrocyclic products are obtained with higher yields (68−91%, see Figure 8b), in comparison to those obtained with the homogeneous catalyst (11−74%). The system is notably efficient in the closure of large rings (>24-membered ones, 91% yield), with a good correlation between pore and substrate size. In order to investigate the factors responsible for the selectivity in the RCM, several MCF-supported catalysts with different pore size, loading of anchored catalyst and linker length were designed and tested. Reducing the amount of the empty space in the pores (overcrowded surroundings, higher catalyst loading, use of non-porous material with lower surface area) decreases reaction efficiency and rate, lowering the selectivity. Increasing the linker length causes lower yields too, which is ascribed to a fast decomposition of the catalyst through the formation of bimetallic adducts.

Subsequently, Buchmeiser, Tallarek et al. extensively studied RCM reactions promoted by diverse Ru-based olefin metathesis catalysts embedded in mesoporous silica, both in batch [57−59] and in flow conditions [60]. Their design reckoned on the selective anchoring of the catalyst to the inner walls of the pores into which just one substrate molecule could be hosted (1:1 stoichiometry with the catalyst). Their expectations have been fulfilled and high macro(-mono)cyclization/oligomerization ratios (MMC/O ratio) have been obtained, even employing relatively high substrate concentrations (up to 25 mM). More in detail (Figure 8c), the heterogeneous catalyst is prepared by initially clogging the silica pores with an α,ω-dihydroxypolyethyleneglycol derivative (Pluronic®). The external hydroxyls are capped with trimethylsilyl groups (Figure 8c). Pluronic® filler is then removed (Soxhlet extraction), providing the mesoporous material with free internal OH groups, onto which the catalyst can be eventually anchored. This procedure ensures the presence of the catalyst inside the pores exclusively.

In an initial work [57], this protocol is applied to the functionalization of two mesoporous silica materials of different pore diameters, namely **SBA1** and **SBA2** (SBA= Santa Barbara Amorphous, with a diameter of 50 and 62 Å, respectively), with RCM catalyst **14** to have catalytic materials **14@SBA1** and **14@SBA2** (Figure 8c). Further functionalization of the remaining free internal hydroxyls with apolar dimethoxydimetylsilane (DMDMS) leads to catalytic materials with additional reduction of pore diameter and local polarity, **14@SBA1d** and **14@SBA2d** respectively (Figure 8d). All materials show higher performances compared to the homogeneous catalyst in terms of MMC/O ratio, which is as high as 2.1 with **14@SBA1d** (MMC/O < 1 in the presence of homogeneous **14**). The best results are achieved by combining the substrates with the highest hydrodynamic radius and **14@SBA1d** the supported catalyst with the smallest pore size (Figure 8d).

Later, the same group reported a related mesoporous silica-supported Mo-based catalyst with improved substrate conversion and MMC/O selectivity (88% and 49, respectively), which operates at even higher substrate concentration (5-fold increase) [59]. In this case, the catalytic sites are directly fixed on the silica support (no spacer). Remarkably, these catalysts show improved E/Z

selectivity compared to the unsupported one (53% vs 33% of Z isomer).

Besides silica materials, Buchmeiser, Lotsch et al. designed a Ru-based metathesis catalyst immobilized inside a mesoporous covalent organic framework (COF) [61], which displayed good selectivity in terms of MMC/O in RCM reaction of α-ω dienes when compared to the corresponding homogeneous catalyst. However, substrate conversion is lower than the silica-based systems [56–60] due to the poor diffusion of the substrate molecules inside the material, an issue that becomes more pronounced as the hydrodynamic ratio of the substrates increases.

In 2020, Myongsoo Lee et al. obtained a series of macrocycles in quantitative yields via Suzuki–Miyaura couplings and Knoevenagel condensations, taking advantage of the confined space provided by self-assembled porous structures [62]. Compound **15** is able to self-assemble into a single-layered porous structure with hexagonal hydrophobic cavities, organized in discrete nanosheets thanks to the presence of oligoether chains that prevent multilayer self-aggregation (Figure 8e). The pores have a diameter of ~2 nm and can host linear substrates **S17** and **S18** with hydrodynamic diameters of 2 nm and 1.9 nm, respectively (Figure 8f). The high efficiency (>95%) in **S17** and **S18** inclusion is not only due to hydrophobic interactions but also to the size matching between substrates and pores. In fact, no incorporation was observed for substrates **S19** and **S20**, which display lower (1.3 nm) and higher (2.3 nm) diameters, respectively. Suzuki–Miyaura intramolecular coupling of **S17** and **S18** is achieved after 4 h at room temperature affording the corresponding macrocycles **P17** and **P18** in quantitative yields (Figure 8f), while mainly oligomers are obtained from **S19** and **S20**, and only ~1% of **P19** and **P20** after 48 h increasing the temperature to 75 °C. Notably, macrocyclization products **P17** and **P18** were spontaneously released from the nanosheets since their size did not match anymore with the pores' diameter, allowing for several catalytic turnovers without any degradation of the material and loss of efficiency.

Conclusion

Along this review, we have shown that confinement within a limited nano-sized space can contribute a great deal to improve several features of cyclization reactions. In particular, in the formation of common rings, different or much higher regio- or stereo-selectivities can be obtained with respect to (natural) bulk conditions, opening new synthetic routes. This is especially true for multi-cyclization reactions carried out with one-(nano)pot procedures. In the case of medium and large cycles, which are always difficult to obtain in bulk solution due to low EM and the consequent necessity of high dilution conditions, confinement in a molecular-sized reactor seems to be an optimal solution, since the otherwise insoluble issue of the competition between cyclization and intermolecular reaction is removed. Thanks to this resource, cyclization reactions to obtain medium and large cyclic products can be carried out at relatively high substrate concentrations, even on preparative scale, avoiding the use of excessive solvent amounts.

In the near future, cyclization procedures that take advantage of the confined space of nanoreactors are expected to be increasingly adopted in the design of synthetic routes involving cyclic intermediates or targets.

Funding

This work was funded by University of Rome La Sapienza (Progetti di Ricerca, Ateneo 2020, RM12017293222D84).

Declaration of competing interest

The authors declare that they have no known competing financial interests or personal relationships that could have appeared to influence the work reported in this paper.

Data availability

Data will be made available on request.

References

Papers of particular interest, published within the period of review, have been highlighted as:

** of outstanding interest

1. McNaught AD, Wilkinson A: *Cyclization*. Oxford: Blackwell Scientific Publications; 1997, https://doi.org/10.1351/goldbook.c01494.

2. Carey FA, Sundberg RJ: *Advanced organic chemistry*. 5th ed. New York, USA: Springer Science + Business Media, LLC; 2007.

3. Di Stefano S, Mandolini L: **The canonical behavior of the entropic component of thermodynamic effective molarity. An attempt at unifying covalent and noncovalent cyclizations**. *Phys Chem Chem Phys* 2019, **21**:955–987, https://doi.org/10.1039/C8CP06344C.

4. Mandolini L: **Intramolecular reactions of chain molecules**. *Adv Phys Org Chem* 1986, **22**:1–111, https://doi.org/10.1016/S0065-3160(08)60167-7.

5. Kirby AJ: **Effective molarities for intramolecular reactions**. In Gold V, Bethell D. *Adv. Phys. Org. Chem.*, vol. 17. Academic Press; 1980:183–278, https://doi.org/10.1016/S0065-3160(08)60129-X.

6. $EM_{equilibrium} = K_{intra}/K_{inter}$. K_{intra} (pure number) is the equilibrium constant for the cyclization of a bifunctional compound A—B, and K_{inter} (measured in M^{-1}) is the equilibrium constant for the corresponding model reaction between monofunctional reactants —A and B—.

7. Di Stefano S, Ercolani G: **Equilibrium effective molarity as a key concept in ring-chain equilibria, dynamic combinatorial chemistry, cooperativity and self-assembly**. *Adv Phys Org Chem* 2016, **50**:1–76, https://doi.org/10.1016/bs.apoc.2016.07.002.

8. Motloch P, Hunter CA: **Thermodynamic effective molarities for supramolecular complexes**. *Adv Phys Org Chem* 2016, **50**: 77–118, https://doi.org/10.1016/bs.apoc.2016.07.001.

9. ** Cacciapaglia R, Di Stefano S, Mandolini L: **Effective molarities in supramolecular catalysis of two-substrate reactions**. *Acc Chem Res* 2004, **37**:113–122, https://doi.org/10.1021/ar020076v.
Here, a critical analysis of EM in catalytic reactions is reported.

10. Di Stefano S, Cacciapaglia R, Mandolini L: **Supramolecular control of reactivity and catalysis – effective molarities of recognition-mediated bimolecular reactions**. *Eur J Org Chem* 2014, **2014**:7304–7315, https://doi.org/10.1002/ejoc.201402690.

11. Prelog V, Frenkiel L, Kobelt M, Barman P: **Zur Kenntnis des Kohlenstoffringes. Ein Herstellungsverfahren für vielgliedrige Cyclanone**. *Helv Chim Acta* 1947, **30**:1741–1749, https://doi.org/10.1002/hlca.19470300637.

12. O'Maille PE, Chappell J, Noel JP: **Biosynthetic potential of sesquiterpene synthases: alternative products of tobacco 5-epi-aristolochene synthase**. *Arch Biochem Biophys* 2006, **448**: 73–82, https://doi.org/10.1016/j.abb.2005.10.028.

13. Lesburg CA, Zhai G, Cane DE, Christianson DW: **Crystal structure of pentalenene synthase: mechanistic insights on terpenoid cyclization reactions in biology**. *Science (80-)* 1997, **277**:1820–1824, https://doi.org/10.1126/science.277.5333.1820.

14. Starks CM, Back K, Chappell J, Noel JP: **Structural basis for cyclic terpene biosynthesis by tobacco 5-epi-aristolochene synthase**. *Science (80-)* 1997, **277**:1815–1820, https://doi.org/10.1126/science.277.5333.1815.

15. Shenoy SR, Pinacho Crisóstomo FR, Iwasawa T, Rebek J: **Organocatalysis in a synthetic receptor with an inwardly directed carboxylic acid**. *J Am Chem Soc* 2008, **130**: 5658–5659, https://doi.org/10.1021/ja801107r.

16. Yu Y, Yang JM, Rebek J: **Molecules in confined spaces: reactivities and possibilities in cavitands**. *Chem* 2020, **6**: 1265–1274, https://doi.org/10.1016/j.chempr.2020.04.014.

17. Pinacho Crisóstomo FR, Lledó A, Shenoy SR, Iwasawa T, Rebek J: **Recognition and organocatalysis with a synthetic cavitand receptor**. *J Am Chem Soc* 2009, **131**:7402–7410, https://doi.org/10.1021/ja900766b.

18. Wang ZJ, Brown CJ, Bergman RG, Raymond KN, Toste FD: **Hydroalkoxylation catalyzed by a gold(I) complex encapsulated in a supramolecular host**. *J Am Chem Soc* 2011, **133**: 7358–7360, https://doi.org/10.1021/ja202055v.

19. ** Hart-Cooper WM, Clary KN, Toste FD, Bergman RG, Raymond KN: **Selective monoterpene-like cyclization reactions achieved by water exclusion from reactive intermediates in a supramolecular catalyst**. *J Am Chem Soc* 2012, **134**:17873–17876, https://doi.org/10.1021/ja308254k.
This is a key pioneering example of altering the selectivity of a cyclization reaction by confining the reaction inside a molecular host.

20. Hastings CJ, Bergman RG, Raymond KN: **Origins of large rate enhancements in the Nazarov cyclization catalyzed by supramolecular encapsulation**. *Chem Eur J* 2014, **20**:3966–3973, https://doi.org/10.1002/chem.201303885.

21. Hastings CJ, Pluth MD, Bergman RG, Raymond KN: **Enzymelike catalysis of the Nazarov cyclization by supramolecular encapsulation**. *J Am Chem Soc* 2010, **132**:6938–6940, https://doi.org/10.1021/ja102633e.

22. Kaphan DM, Toste FD, Bergman RG, Raymond KN: **Enabling new modes of reactivity via constrictive binding in a supramolecular-assembly-catalyzed aza-prins cyclization**. *J Am Chem Soc* 2015, **137**:9202–9205, https://doi.org/10.1021/jacs.5b01261.

23. Takezawa H, Fujii Y, Murase T, Fujita M: **Electrophilic spirocyclization of a 2-biphenylacetylene via conformational fixing within a hollow-cage host**. *Angew Chem Int Ed* 2022, **61**, e202203970, https://doi.org/10.1002/anie.202203970.

24. ** Zhang Q, Tiefenbacher K: **Terpene cyclization catalysed inside a self-assembled cavity**. *Nat Chem* 2015, **7**:197–202, https://doi.org/10.1038/nchem.2181.
This is a key example of efficient terpene cyclization via nanoconfinement.

25. Zhang Q, Tiefenbacher K: **Hexameric resorcinarene capsule is a brønsted acid: investigation and application to synthesis and catalysis**. *J Am Chem Soc* 2013, **135**:16213–16219, https://doi.org/10.1021/ja4080375.

26. Zhang Q, Catti L, Pleiss J, Tiefenbacher K: **Terpene cyclizations inside a supramolecular catalyst: leaving-group-controlled product selectivity and mechanistic studies**. *J Am Chem Soc* 2017, **139**:11482–11492, https://doi.org/10.1021/jacs.7b04480.

27. Merget S, Catti L, Piccini G, Tiefenbacher K: **Requirements for terpene cyclizations inside the supramolecular resorcinarene capsule: bound water and its protonation determine the catalytic activity**. *J Am Chem Soc* 2020, **142**:4400–4410, https://doi.org/10.1021/jacs.9b13239.

28. Catti L, Tiefenbacher K: **Intramolecular hydroalkoxylation catalyzed inside a self-assembled cavity of an enzyme-like host structure**. *Chem Commun* 2015, **51**:892–894, https://doi.org/10.1039/C4CC08211G.

29. Jackson AC, Goldman BE, Snider BB: **Intramolecular and intermolecular Lewis acid catalyzed ene reactions using ketones as enophiles**. *J Org Chem* 1984, **49**:3988–3994, https://doi.org/10.1021/jo00195a022.

30. Catti L, Tiefenbacher K: **Brønsted acid-catalyzed carbonyl-olefin metathesis inside a self-assembled supramolecular host**. *Angew Chem Int Ed* 2018, **57**:14589–14592, https://doi.org/10.1002/anie.201712141.

31. Catti L, Pöthig A, Tiefenbacher K: **Host-catalyzed cyclodehydration–rearrangement cascade reaction of unsaturated tertiary alcohols**. *Adv Synth Catal* 2017, **359**: 1331–1338, https://doi.org/10.1002/adsc.201601363.

32. Zhang Q, Rinkel J, Goldfuss B, Dickschat JS, Tiefenbacher K: **Sesquiterpene cyclizations catalysed inside the resorcinarene capsule and application in the short synthesis of isolongifolene and isolongifolenone**. *Nat Catal* 2018, **1**:609–615, https://doi.org/10.1038/s41929-018-0115-4.

33. Zhang Q, Tiefenbacher K: **Sesquiterpene cyclizations inside the hexameric resorcinarene capsule: total synthesis of δ-selinene and mechanistic studies**. *Angew Chem Int Ed* 2019, **58**:12688–12695, https://doi.org/10.1002/anie.201906753.

34. Tanimoto H, Kiyota H, Oritani T, Matsumoto K: **Stereochemistry of a unique tricarbocyclic compound prepared by superacid-catalyzed cyclization**. *Synlett* 1997, **1**:121–122, https://doi.org/10.1039/d1qo00750e.

35. Syntrivanis L-D, Némethová I, Schmid D, Levi S, Prescimone A, Bissegger F, *et al.*: **Four-step access to the sesquiterpene natural product presilphiperfolan-1β-ol and unnatural derivatives via supramolecular catalysis**. *J Am Chem Soc* 2020, **142**:5894–5900, https://doi.org/10.1021/jacs.0c01464.

36. Díez-González S, Marion N, Nolan SP: **N-heterocyclic carbenes in late transition metal catalysis**. *Chem Rev* 2009, **109**: 3612–3676, https://doi.org/10.1021/cr900074m.

37. ** Guitet M, Zhang P, Marcelo F, Tugny C, Jiménez-Barbero J, Buriez O, *et al.*: **NHC-capped cyclodextrins (ICyDs): insulated metal complexes, commutable multicoordination sphere, and cavity-dependent catalysis**. *Angew Chem Int Ed* 2013, **52**: 7213–7218, https://doi.org/10.1002/anie.201301225.
This is a pioneering examples of controlling the stereoselectivity of cyclization with the cavity chirality and shape.

38. Zhang P, Tugny C, Meijide Suárez J, Guitet M, Derat E, Vanthuyne N, *et al.*: **Artificial chiral metallo-pockets including a single metal serving as structural probe and catalytic center**. *Chem* 2017, **3**:174–191, https://doi.org/10.1016/j.chempr.2017.05.009.

39. Tugny C, del Rio N, Koohgard M, Vanthuyne N, Lesage D, Bijouard K, *et al.*: **β-Cyclodextrin–NHC–Gold(I) complex (β-ICyD)AuCl: a chiral nanoreactor for enantioselective and substrate-selective alkoxycyclization reactions**. *ACS Catal* 2020, **10**:5964–5972, https://doi.org/10.1021/acscatal.0c00127.

40. Zhu X, Xu G, Chamoreau L-M, Zhang Y, Mouriès-Mansuy V, Fensterbank L, *et al.*: **Permethylated NHC-capped α- and β-cyclodextrins (ICyDMe) regioselective and enantioselective gold-catalysis in pure water**. *Chem Eur J* 2020, **26**: 15901–15909, https://doi.org/10.1002/chem.202001990.

41. Giovanardi G, Secchi A, Arduini A, Cera G: **Diametric calix[6]arene-based phosphine gold(I) cavitands**. *Beilstein J Org Chem* 2022, **18**:190–196, https://doi.org/10.3762/bjoc.18.21.

42. Rusali LE, Schramm MP: **Au-Cavitands: size governed arene-alkyne cycloisomerization**. *Tetrahedron Lett* 2020, **61**, 152333, https://doi.org/10.1016/j.tetlet.2020.152333.

43. Cavarzan A, Scarso A, Sgarbossa P, Strukul G, Reek JNH: **Supramolecular control on chemo- and regioselectivity via encapsulation of (NHC)-Au catalyst within a hexameric self-assembled host**. *J Am Chem Soc* 2011, **133**:2848–2851, https://doi.org/10.1021/ja111106x.

44. Cavarzan A, Reek JNH, Trentin F, Scarso A, Strukul G: **Substrate selectivity in the alkyne hydration mediated by NHC–Au(i) controlled by encapsulation of the catalyst within a hydrogen bonded hexameric host**. *Catal Sci Technol* 2013, **3**: 2898–2901, https://doi.org/10.1039/C3CY00300K.

45. Martín-Torres I, Ogalla G, Yang J-M, Rinaldi A, Echavarren AM: **Enantioselective alkoxycyclization of 1,6-enynes with gold(I)-Cavitands: total synthesis of mafaicheenamine C**. *Angew Chem Int Ed* 2021, **60**:9339–9344, https://doi.org/10.1002/anie.202017035.

46. Sokolova D, Piccini G, Tiefenbacher K: **Enantioselective tail-to-head terpene cyclizations by optically active hexameric resorcin[4]arene capsule derivatives**. *Angew Chem Int Ed* 2022, **61**, e202203384, https://doi.org/10.1002/anie.202203384.

47. Zhang Q, Catti L, Tiefenbacher K: **Catalysis inside the hexameric resorcinarene capsule**. *Acc Chem Res* 2018, **51**: 2107–2114, https://doi.org/10.1021/acs.accounts.8b00320.

48. Mosca S, Yu Y, Gavette JV, Zhang K-D, Rebek J: **A deep cavitand templates lactam formation in water**. *J Am Chem Soc* 2015, **137**:14582–14585, https://doi.org/10.1021/jacs.5b10028.

49. Wu N-W, Rebek J: **Cavitands as chaperones for monofunctional and ring-forming reactions in water**. *J Am Chem Soc* 2016, **138**:7512–7515, https://doi.org/10.1021/jacs.6b04278.

50. ** Shi Q, Masseroni D, Rebek J: **Macrocyclization of folded diamines in cavitands**. *J Am Chem Soc* 2016, **138**:10846–10848, https://doi.org/10.1021/jacs.6b06950.
A key example of templating macrocycle formation by inclusion of a linear guest inside a bowl-shaped receptor.

51. Wu N-W, Petsalakis ID, Theodorakopoulos G, Yu Y, Rebek Jr : **J.Cavitands as containers for α,ω-dienes and chaperones for olefin metathesis**. *Angew Chem Int Ed* 2018, **57**:15091–15095, https://doi.org/10.1002/anie.201808265.

52. Yang J-M, Yu Y, Rebek JJ: **Selective macrocycle formation in cavitands**. *J Am Chem Soc* 2021, **143**:2190–2193, https://doi.org/10.1021/jacs.0c12302.

53. Wang K, Cai X, Yao W, Tang D, Kataria R, Ashbaugh HS, *et al.*: **Electrostatic control of macrocyclization reactions within nanospaces**. *J Am Chem Soc* 2019, **141**:6740–6747, https://doi.org/10.1021/jacs.9b02287.

54. Yao W, Wang K, Ismaiel YA, Wang R, Cai X, Teeler M, *et al.*: **Electrostatic potential field effects on amine macrocyclizations within yoctoliter spaces: supramolecular electron withdrawing/donating groups**. *J Phys Chem B* 2021, **125**: 9333–9340, https://doi.org/10.1021/acs.jpcb.1c05238.

55. Ashbaugh HS, Gibb BC, Suating P: **Cavitand complexes in aqueous solution: collaborative experimental and computational studies of the wetting, assembly, and function of nanoscopic bowls in water**. *J Phys Chem B* 2021, **125**: 3253–3268, https://doi.org/10.1021/acs.jpcb.0c11017.

56. Jee JE, Cheong JL, Lim J, Chen C, Hong SH, Lee SS: **Highly selective macrocycle formations by metathesis catalysts fixated in nanopores**. *J Org Chem* 2013, **78**:3048–3056, https://doi.org/10.1021/jo302823w.

57. ** Ziegler F, Teske J, Elser I, Dyballa M, Frey W, Kraus H, *et al.*: **Olefin metathesis in confined geometries: a biomimetic approach toward selective macrocyclization**. *J Am Chem Soc* 2019, **141**:19014–19022, https://doi.org/10.1021/jacs.9b08776.
A prominent example of macrocyclization catalysis exploiting the pores of catalytic materials.

58. Tallarek U, Hochstrasser J, Ziegler F, Huang X, Kübel C, Buchmeiser MR: **Olefin ring-closing metathesis under spatial confinement: morphology–Transport relationships**. *ChemCatChem* 2021, **13**:281–292, https://doi.org/10.1002/cctc.202001495.

59. Ziegler F, Kraus H, Benedikter MJ, Wang D, Bruckner JR, Nowakowski M, *et al.*: **Confinement effects for efficient macrocyclization reactions with supported cationic molybdenum imido alkylidene N-heterocyclic carbene complexes**. *ACS Catal* 2021:11570–11578, https://doi.org/10.1021/acscatal.1c03057.

60. Ziegler F, Roider T, Pyschik M, Haas CP, Wang D, Tallarek U, *et al.*: **Olefin ring-closing metathesis under spatial confinement and continuous flow**. *ChemCatChem* 2021, **13**: 2234–2241, https://doi.org/10.1002/cctc.202001993.

61. Emmerling ST, Ziegler F, Fischer FR, Schoch R, Bauer M, Plietker B, *et al.*: **Olefin metathesis in confinement: towards covalent organic framework scaffolds for increased macrocyclization selectivity**. *Chem Eur J* 2022, **28**, https://doi.org/10.1002/chem.202104108.

62. Liu X, Zhou X, Shen B, Kim Y, Wang H, Pan W, *et al.*: **Porous nanosheet assembly for macrocyclization and self-release**. *J Am Chem Soc* 2020, **142**:1904–1910, https://doi.org/10.1021/jacs.9b11004.